9

## Research Article

Dean Chou, Umair Asghar\*, and Muhammad Imran Asjad

# Computation of exact analytical soliton solutions and their dynamics in advanced optical system

https://doi.org/10.1515/phys-2025-0220 received October 07, 2024; accepted September 28, 2025

**Abstract:** This study explores the modified Benjamin–Bona– Mahony equation using the new extended direct algebraic approach, a powerful analytical technique for solving nonlinear partial differential equations. The proposed methodology yields a diverse spectrum of exact solutions, categorized into 12 distinct classes, including rational, hyperbolic, and trigonometric functions, as well as mixed periodic, singular, shock-singular, complex solitary-shock, and planewave solutions. These solutions are systematically derived and validated using Mathematica, demonstrating the reliability and effectiveness of the method. A comparative analysis with existing techniques underscores the consistency and superiority of the proposed approach. Additionally, the Hamiltonian function is constructed to examine the system's conservation properties, ensuring the physical relevance of the obtained solutions. A comprehensive sensitivity analysis is performed to assess the model response to variations in parameters and initial conditions. To further illustrate the dynamical characteristics of the solutions, three-dimensional, two-dimensional, and contour plots are presented, offering deeper insights into their physical behavior. The results contribute to the larger study of nonlinear wave phenomena in engineering and applied sciences, providing a robust analytical framework for future research in soliton theory and mathematical physics.

**Keywords:** modified Benjamin–Bona–Mahony equation, Hamiltonian function, new extended direct algebraic approach, sensitive assessment

**Dean Chou:** Department of Biomedical Engineering, National Cheng Kung University, Tainan 701401, Taiwan; Academy of Innovative Semiconductor and Sustainable Manufacturing, National Cheng Kung University, Tainan 701401, Taiwan

**Muhammad Imran Asjad:** Department of Mathematics, University of Management and Technology, Lahore, Pakistan; Jadara Research Center, Jadara University, Irbid 21110, Jordan

#### 1 Introduction

The most important component of investigating nonlinear physical mechanisms is looking into traveling wave solutions to nonlinear partial differential equations (NPDEs) that can be developed around the areas of engineering sciences, mathematics, and technological fields. Nonlinear partial differential equations (NPDEs), including partial differential equations (PDEs) and ordinary differential equations (ODEs), play a crucial role in modeling significant phenomena in various scientific fields such as chemistry, engineering, biology, and finance. They are also widely used to describe the physical properties of different models, as discussed in refs. [1-5]. Nonlinear partial differential equations (NPDEs) have been extensively employed to model significant phenomena and dynamic advancements across various scientific and engineering fields in recent years [6-8]. Hence, it is also used to describe the intricate characteristics in these sectors and to help researchers use them to achieve the most important objective and systematic advancements. To understand the course of numerous physical occurrences, the solitary wave formulations of these kinds of structures play a crucial role. The wave processes of dispersion, dissipation, diffusion, response, and convection are important in nonlinear wave equations [9,10]. Ocean engineering, solitary wave theory, tsunami waves, water waves, hydrodynamics, optical fibers, turbulence theory, chemical physics, chaos theory, and several other domains are just a few examples of the many applications in which nonlinear evolution equations (NLEEs) are utilized [11,12]. These types of models have become common in several fields, such as physics, practical mathematics, and engineering sciences, and may be used to investigate a wide variety of nonlinear events that occur in real life [13-19].

At that time, numerous writers who were interested in nonlinear physical processes looked into the nonlinear evolution equation's exact solution. Plenty of scientists and mathematicians have developed and used some significant methods.

The Benjamin–Bona–Mahony (BBM) equation is as follows:

$$K_t + K_x + KK_x + K_{xxt} = 0.$$
 (1)

<sup>\*</sup> Corresponding author: Umair Asghar, Department of Mathematics, University of Management and Technology, Lahore, Pakistan, e-mail: umairas926@gmai.com

It was initially developed to represent a surface long-wave approximation in a nonlinear dispersive medium. This equation additionally applies to acoustic-gravity waves of compressed water, enharmonic crystal acoustic waves, and cold plasma hydromagnetic waves. Rogue waves in the water have been studied using its Peregrine soliton theories plus its BBM equation. However, rogue waves present a serious hazard to ships and offshore infrastructure. The study of rogue waves in the water has made use of the BBM equation and the Peregrine soliton idea. However, rogue waves can damage ships, including offshore infrastructure. Freak waves are abnormally enormous ocean waves that suddenly arise and can rise significantly higher above the waves around them. These waves have been seen in a variety of bodies of water, such as lakes, seas, and especially oceans. For coastal regions, offshore structures and marine activities pose major risks. In addition to being created by Peregrine, the BBM equation is another name for the regularized long-wave equation.

In this article, we take into consideration the modified BBM equation as follows.

$$K_t + K_x + jK^nK_x + \ell K_{xxt} = 0.$$
 (2)

When n = 1, Eq. (2) is known as the BBM equation, which is seen as an advancement over the KdV equation, while can be utilized as an explanation for the long surface gravity wave's characteristics, hydromagnetic waves with freezing plasma plus acoustic-gravity waves for compressible fluids likewise, the sound waves through a harmonic crystal [20,21].

When n = 2, we have a modified BBM equation, Eq. (2). Additionally, this is employed throughout the study of optical illusions, which employs color and light together with patterning. Pictures that can trick our minds are made using certain components, like those of Sun *et al.* and Coclite *et al.* [22,23],

$$K_t + K_x + jK^2K_x + \ell K_{xxt} = 0,$$
 (3)

where K(x,t) is a given function, j and  $\ell$  are nonzero and real constants, and Eq. (3) is dependent upon the value of n. To replicate a long surface gravity wave having tiny magnitudes spreading in a (1+1) dimension, the modified equation was presented. We employ a powerful and practical method for creating many other soliton solutions for the modified BBM equation. The new extended direct algebraic approach [24,25] is used in the construction of the traveling wave solutions to the modified Benjamin–Bona–Mahony (mBBM) equation. The modification in the mBBM equation compared to the mBBM equation allows for the consideration of additional effects or parameters, making it more versatile in describing the behavior of certain types of waves. The study of solutions to the mBBM equation provides insights into the complex dynamics of dispersive

waves and their interactions. The physical significance of the mBBM equation lies in its ability to model and describe the behavior of certain types of water waves, incorporating both nonlinear and dispersive effects. The mBBM equation is a NPDE, and its study falls within the broader context of nonlinear science. Understanding the solutions to such equations contributes to our knowledge of nonlinear phenomena, which is relevant in various scientific disciplines beyond fluid dynamics. On comparing with other methods, the proposed method is advanced and new, and by using it we can obtain various kinds of results.

To give exact traveling wave solutions for NPDEs. many researchers have recently developed a variety of techniques. For example, the auxiliary expansion method [26,27], extended direct algebraic methodology, the tanh and extended tanh method [28], the expension  $\frac{G'}{G}$  methodology [29], extended Fan sub-equation methodology [30], sine-cosine methodology, Jacobi elliptic function method [31,32], algebraic method [33], variational method, Darboux transformation, Hirota method, function transformation method, Lie group analysis, extended simple equation method [34-37], the tanh-coth method, and the sn-ns method [38], Hirota's bilinear method [39], bifurcation analysis [40], mapping method [41], Jacobi elliptic function method [42], and multiple exponential-function approach [43]. The space-time fractional potential Kadomtsev-Petviashvili equation with the space-time fractional mBBM equation may both be solved using the modified Kudryashov method, according to Ege and Misirli [44], extended F-expansion method [45], modified extended tanh-function method [46-48], and modified extended direct algebraic method [49]. For such NPDEs, the generalized Kudryashov approach was employed to provide a traveling wave method. More research is necessary for the numerical analysis of the space-time mBBM-type equations after reviewing these advancements.

The primary motivation of this study is to derive traveling wave solutions for the mBBM equation, a fundamental NPDE that arises in various physical and engineering applications, including fluid dynamics, shallow water wave theory, nonlinear optics, and plasma physics. While numerous researchers have employed different analytical and numerical techniques to solve this equation, the new extended direct algebraic approach presents a novel and powerful alternative, yielding previously undiscovered solutions. This advanced method not only enhances the depth of analysis but also provides new insights unattainable through conventional approaches, making it a valuable tool in the study of nonlinear wave phenomena. The proposed methodology generates a diverse range of

exact solutions, categorized into 12 distinct classes, each offering unique mathematical and physical interpretations. These include rational, hyperbolic, and trigonometric function-based solutions, as well as mixed periodic, singular, and shock-singular solutions, which highlight critical transitions and singular behaviors within the system. The study also uncovers mixed complex solitary-shock solutions, integrating solitary wave dynamics with shock wave effects, further expanding the understanding of nonlinear wave interactions. Additionally, mixed trigonometric, mixed hyperbolic, and mixed plane wave solutions provide a broader perspective on the interplay between different functional structures. We also perform a dynamic investigation for deep understanding. To check the reliability of the model we also perform the sensitivity analysis. The classification of these solutions significantly enhances the comprehension of the underlying dynamics of the mBBM equation, facilitating its application in real-world scenarios. In optical fiber communication, they aid in the study of pulse transmission in nonlinear media, ensuring stable signal propagation. It is also very useful in the advanced optical system which refers to modern optical communication and photonic structures where soliton dynamics play a crucial role. These systems include optical fiber networks, photonic crystals, nonlinear waveguides, and signal processing technologies that utilize soliton solutions for efficient data transmission and wave propagation. By providing a comprehensive framework for exploring the mBBM equation, this study lays the foundation for future advancements in applied mathematics, engineering, and physics, enabling further theoretical and practical developments in nonlinear wave theory.

PDEs have attracted the attention of technologists along with biological scholars due to their utility in modeling a range of scientific processes in diverse fields, including signals alongside the processing of images, mathematically based mechanical work, and biochemistry, which are all areas of study. Because most physical systems are nonlinear, scientists have been exploring the conditions under which precise solutions to nonlinear partial differential equations (NLPDEs), in particular nonlinear evolution equations (NLEEs), can be obtained. Obtained new solutions to NLPDEs can considerably enhance our understanding of their physical significance, consistent with the findings reported by Shakeel et al. [50]. As in nonlinear physical phenomena, different solitons have been recognized as fundamental components that characterize the dynamical characteristics of interacting things, particularly in studies of nonlinear optical fiber, electromagnetic wave propagation via communicating charged plasma, especially their occurrence in gravitational waves,

which consolidate their significance from a mathematical alongside physical points of view [51].

This article is organized as Section 2, clarification about methods, along with an overview. Section 3 provides the construction of the soliton solutions as well as describes the graphic depiction. An illustrated description is presented in Section 4. Section 5 describes the sensitivity analysis to verify the model's sensitivity aspects, and finally. Section 6 provides the conclusion.

## 2 Explanation of the analytical method

The suggested approaches are successfully pertinent to complex nonlinear dominant structures.

Consider a general non-linear partial differential equation:

$$\mathcal{A}(K, K_{Y}, K_{t}, K_{Yt}, K_{YY}, ...) = 0,$$
 (4)

where  $\mathcal{A}$  is the polynomial in K = K(x, t) is an unspecified function and it's partial derivatives.

That converts through the ODE:

$$\mathcal{B}(\mathbb{D}, \mathbb{D}', \mathbb{D}'', ...) = 0. \tag{5}$$

Apply the transformation given

$$K(x,t) = \mathbb{D}(\vartheta),$$
 (6)

where  $\vartheta = \mu x - \nu t$ .

## 3 Application of new extended direct algebraic methodology

To determine the exact analytical solution of the solitary wave of the mBBM equation, a new extended direct algebraic method will be applied [52]. Let us use Eq. (3) due to its generality. We have

$$(\mu - \nu)K'(\vartheta) + \mathcal{J}\mu K^2(\vartheta)K' - \mu^2 \nu \ell K'''(\vartheta) = 0.$$
 (7)

Integrating Eq. (7) with regard to  $\vartheta$  and the constant is zero,

$$(\mu - \nu)K(\vartheta) + \frac{1}{3}j\mu K^3(\vartheta) - \mu^2 \nu \ell K''(\vartheta) = 0.$$
 (8)

A solution of Eq. (8) is adjusted by a homogeneous balance parameter

$$K(\vartheta) = e_0 + e_1(\mathbb{G}(\vartheta)). \tag{9}$$

By substituting the proposed solution from Eq. (9) into Eq. (8) and equating the coefficients of different powers,

we obtain the corresponding algebraic system of equations.

$$G(\vartheta)^{0} : \mu e_{0} - \nu e_{0} + 1/3 j \mu e_{0}^{3} - \mu^{2} \nu \ell e_{1} \varpi(\ln(Q))^{2} \rho,$$

$$G(\vartheta)^{1} : \mu e_{1} - \nu e_{1} + j \mu e_{0}^{2} e_{1} - \mu^{2} \nu \ell e_{1} \varpi^{2} (\ln(Q))^{2}$$

$$- 2\mu^{2} \nu \ell e_{1} \lambda (\ln(Q))^{2} \rho,$$

$$G(\vartheta)^{2} : j \mu e_{0} e_{1}^{2} - 3\mu^{2} \nu \ell e_{1} \varpi(\ln(Q))^{2} \lambda,$$

$$G(\vartheta)^{3} : 1/3 j \mu e_{1}^{3} - 2\mu^{2} \nu \ell e_{1} \lambda^{2} (\ln(Q))^{2}.$$
(10)

The solution of upper model Eq. (10) is acquired with the support of Mathematica

$$\begin{bmatrix} e_0 = \pm \sqrt{3} \Gamma \ln(Q) \mu \varpi, & e_1 = \pm 2\sqrt{3} \Gamma \ln(Q) \mu \lambda, \\ v = \pm \frac{2\mu}{2 - \mu^2 \ln(Q)^2 \ell \Pi} \end{bmatrix}, \tag{11}$$

where

$$\Gamma = \sqrt{\frac{\ell}{j[2 - \ell\mu^2 \ln(Q)^2 \Pi]}}, \quad \Pi = \varpi^2 - 4\rho\lambda. \quad (12)$$

Substituting Eq. (11) in Eq. (9) for a general solution to Eq. (1)

$$K(x,t) = \pm \sqrt{3} \Gamma \ln(Q) \mu \varpi \pm 2\sqrt{3} \Gamma \ln(Q) \mu \lambda(\mathbb{G}(\vartheta)). \quad (13)$$

(Class 1): As  $\varpi^2$  –  $4\rho\lambda$  < 0, as well as  $\lambda \neq 0$ , following that, mixed trigonometric solutions can be acquired,

$$K_1(x,t) = \sqrt{3}\Gamma \ln(Q)\mu\sqrt{-\Pi} \tan_Q \left(\frac{\sqrt{-\Pi}}{2}\vartheta\right), \qquad (14)$$

$$K_2(x,t) = -\sqrt{3} \Gamma \ln(Q) \mu \sqrt{-\Pi} \cot_Q \left[ \frac{\sqrt{-\Pi}}{2} \vartheta \right], \quad (15)$$

$$K_3(x, t) = \sqrt{3} \Gamma \ln(Q) \mu \sqrt{-\Pi} \left( \tan_Q(\sqrt{-\Pi} \vartheta) \right)$$

$$\pm \sqrt{mn} \sec_Q(\sqrt{-\Pi} \vartheta),$$
(16)

$$K_4(x,t) = \sqrt{3} \Gamma \ln(Q) \mu \sqrt{-\Pi} \left( \cot_Q(\sqrt{-\Pi} \vartheta) \right)$$

$$\pm \sqrt{mn} \csc_Q(\sqrt{-\Pi} \vartheta),$$
(17)

$$K_{5}(x,t) = \frac{\sqrt{3}}{2} \Gamma \ln(Q) \mu \varpi \sqrt{-\Pi} \left[ \tan_{Q} \left( \frac{\sqrt{-\Pi}}{4} \vartheta \right) \right] - \cot_{Q} \left( \frac{\sqrt{-\Pi}}{4} \vartheta \right) \right].$$
(18)

(Class 2): As  $\varpi^2 - 4\rho\lambda > 0$ , as well as  $\lambda \neq 0$ , we obtained the solutions of various kinds as follows.

Shock solution is achieved as

$$K_6(x,t) = -\sqrt{3}\Gamma \ln(Q)\mu\sqrt{\Pi} \tanh_Q \left(\frac{\sqrt{\Pi}}{2}\vartheta\right). \tag{19}$$

The singular outcome is derived as

$$K_6(x,t) = -\sqrt{3}\Gamma \ln(Q)\mu\sqrt{\Pi} \coth_Q \left(\frac{\sqrt{\Pi}}{2}\vartheta\right). \tag{20}$$

A mixed complex solitary wave outcome is acquired as

$$K_7(x,t) = \sqrt{3} \Gamma \ln(Q) \mu \sqrt{\Pi} \left( -\tanh_Q(\sqrt{\Pi} \vartheta) \right)$$

$$\pm i \sqrt{mn} \operatorname{sech}_O(\sqrt{\Pi} \vartheta).$$
(21)

The mixed singular outcome is within the shape of

$$K_8(x,t) = \sqrt{3} \Gamma \ln(Q) \mu \sqrt{\Pi} \left( -\coth_Q(\sqrt{\Pi} \vartheta) \right)$$

$$\pm \sqrt{mn} \operatorname{csch}_Q(\sqrt{\Pi} \vartheta) \right). \tag{22}$$

The mixed shock singular outcomes are achieved along with the shape of

$$K_{9}(x,t) = -\frac{\sqrt{3}}{2}\Gamma\ln(Q)\mu\sqrt{\Pi}\left\{\tanh_{Q}\left(\frac{\sqrt{\Pi}}{4}\vartheta\right)\right\} + \coth_{Q}\left(\frac{\sqrt{\Pi}}{4}\vartheta\right)\right\}. \tag{23}$$

(Class 3): As  $\rho\lambda > 0$  as well as  $\varpi = 0$ , the trigonometric result is

$$K_{11}(x,t) = 2\sqrt{3}\sqrt{\frac{\ell}{2j(1+2\ell\mu^2\ln(Q)^2\lambda\rho)}}\ln(Q)\mu$$

$$\times \sqrt{\lambda\rho}\left((\tan_{Q}(\lambda\vartheta))\right),$$
(24)

$$K_{12}(x,t) = -2\sqrt{3}\sqrt{\frac{\ell}{2\dot{j}(1+2\ell\mu^2\ln(Q)^2\lambda\rho)}}\ln(Q)\mu\sqrt{\lambda\rho}$$

$$\times ((\cot_Q(\lambda\vartheta))). \tag{25}$$

The mixed trigonometric results are derived as

$$K_{13}(x,t) = 2\sqrt{3} \sqrt{\frac{\ell}{2j(1 + 2\ell\mu^2 \ln(Q)^2 \lambda \rho)}} \ln(Q)\mu$$

$$\times \sqrt{\lambda \rho} \left( \tan_Q(2\sqrt{\rho\lambda} \vartheta) \right)$$

$$\pm \sqrt{mn} \sec_Q(2\sqrt{\rho\lambda} \vartheta)),$$
(26)

$$K_{14}(x,t) = 2\sqrt{3} \sqrt{\frac{\ell}{2j(1 + 2\ell\mu^2 \ln(Q)^2 \lambda \rho)}} \ln(Q)\mu$$

$$\times \sqrt{\lambda \rho} \left(-\cot_Q(2\sqrt{\rho\lambda}\vartheta)\right)$$

$$\pm \sqrt{mn} \csc_Q(2\sqrt{\rho\lambda}\vartheta),$$
(27)

$$K_{15}(x,t) = \sqrt{3} \sqrt{\frac{\ell}{2j(1 + 2\ell\mu^{2} \ln(Q)^{2}\lambda\rho)}} \ln(Q)\mu\sqrt{\lambda\rho}$$

$$\times \left[ \tan_{Q} \left( \frac{\sqrt{\rho\lambda}}{2} \vartheta \right) - \cot_{Q} \left( \frac{\sqrt{\rho\lambda}}{2} \psi \right) \right]. \tag{28}$$

(Class 4): As  $\rho\lambda$  < 0 as well as  $\varpi$  = 0, solutions within the shape of shock soliton are obtained as

$$K_{16}(x,t) = -2\sqrt{3}\iota\sqrt{\frac{\ell}{2j(1+2\ell\mu^2\ln(Q)^2\lambda\rho)}}\ln(Q)\mu$$

$$\times \sqrt{\lambda\rho}\tanh_{Q}(\sqrt{-\rho\lambda}\vartheta). \tag{29}$$

We obtain the singular solution as

$$K_{17}(x,t) = -2\sqrt{3}\iota\sqrt{\frac{\ell}{2j(1+2\ell\mu^2\ln(Q)^2\lambda\rho)}}\ln(Q)\mu$$

$$\times \sqrt{\lambda\rho} \coth_{Q}(\sqrt{-\rho\lambda}\vartheta).$$
(30)

The distinct solutions of complex combo type derived as

$$\begin{split} K_{18}(x,t) &= 2\sqrt{3}\,\iota\sqrt{\frac{\ell}{2\dot{\varphi}(1+2\ell\mu^2\ln(Q)^2\lambda\rho)}}\,\ln(Q)\mu\sqrt{\lambda\rho} \\ &\times (-\tanh_Q(2\sqrt{-\rho\lambda}\,\vartheta) \\ &\pm \sqrt{mn}\,\mathrm{sech}_Q(2\sqrt{-\rho\lambda}\,\vartheta)), \end{split} \tag{31}$$

$$K_{19}(x,t) = 2\sqrt{3} \iota \sqrt{\frac{\ell}{2j(1 + 2\ell\mu^2 \ln(Q)^2 \lambda \rho)}} \ln(Q)\mu \sqrt{\lambda \rho}$$

$$\times (-\coth_Q(2\sqrt{-\rho\lambda}\vartheta))$$

$$\pm \sqrt{mn}\operatorname{csch}_Q(2\sqrt{-\rho\lambda}\vartheta)),$$
(32)

$$K_{20}(x,t) = -\sqrt{3} \iota \sqrt{\frac{\ell}{2j(1 + 2\ell\mu^2 \ln(Q)^2 \lambda \rho)}} \ln(Q)\mu \sqrt{\lambda \rho}$$

$$\times \left[ \tanh_Q \left[ \frac{\sqrt{-\rho\lambda}}{2} \vartheta \right] + \coth_Q \left[ \frac{\sqrt{-\rho\lambda}}{2} \vartheta \right] \right]. \tag{33}$$

(Class 5): As  $\rho = \lambda$  and  $\varpi = 0$ , the periodic along with mixed periodic solutions could be acquired in the configuration of periodic and mixed periodic class

$$K_{21}(x,t) = 2\sqrt{3}\sqrt{\frac{\ell}{2j(1+2\ell\mu^2\ln(Q)^2\lambda^2)}}\ln(Q)\mu$$

$$\times \lambda((\tan_Q(\lambda\vartheta))), \tag{34}$$

$$K_{22}(x,t) = -2\sqrt{3} \sqrt{\frac{\ell}{2\ell(1 + 2\ell\mu^2 \ln(Q)^2 \lambda^2)}} \ln(Q)\mu \times \lambda((\cot_Q(\rho\theta))),$$
(35)

$$K_{23}(x,t) = 2\sqrt{3} \sqrt{\frac{\ell}{2j(1 + 2\ell\mu^2 \ln(Q)^2\lambda^2)}} \ln(Q)\mu$$

$$\times \lambda((\tan_Q(2\lambda\vartheta) \pm \sqrt{mn} \sec_Q(2\lambda\vartheta))),$$
(36)

$$K_{24}(x,t) = 2\sqrt{3} \sqrt{\frac{\ell}{2j(1 + 2\ell\mu^2 \ln(Q)^2\lambda^2)}} \ln(Q)\mu$$

$$\times \lambda((-\cot_Q(2\lambda\vartheta) \pm \sqrt{mn} \csc_Q(2\lambda\vartheta))),$$
(37)

$$K_{25}(x,t) = \sqrt{3} \sqrt{\frac{\ell}{2j(1 + 2\ell\mu^2 \ln(Q)^2 \lambda^2)}} \ln(Q)\mu$$

$$\times \lambda \left[ \tan_Q \left( \frac{\lambda}{2} \vartheta \right) - \cot_Q \left( \frac{\lambda}{2} \vartheta \right) \right]. \tag{38}$$

(Class 6): As  $\varpi = 0$  and  $\lambda = -\rho$ , single as well as mixed wave composition is obtained within the following class:

$$K_{26}(x,t) = 2\sqrt{3}\sqrt{\frac{\ell}{2j(1-2\ell\mu^2\ln(Q)^2\rho^2)}}\ln(Q)\mu$$

$$\times \rho(\tanh_Q(\rho\vartheta)),$$
(39)

$$K_{27}(x,t) = 2\sqrt{3}\sqrt{\frac{\ell}{2j(1-2\ell\mu^2\ln(Q)^2\rho^2)}}\ln(Q)\mu \qquad (40)$$
$$\times \rho(\coth_{Q}(\rho\vartheta)),$$

$$K_{28}(x,t) = -2\sqrt{3}\sqrt{\frac{\ell}{2j(1-2\ell\mu^2\ln(Q)^2\rho^2)}}\ln(Q)\mu\rho$$

$$\times (-\tanh_Q(2\rho\vartheta) \pm \iota\sqrt{mn}\operatorname{sech}_Q(2\rho\vartheta)),$$
(41)

$$K_{29}(x,t) = -2\sqrt{3}\sqrt{\frac{\ell}{2j(1-2\ell\mu^2\ln(Q)^2\rho^2)}}\ln(Q)\mu\rho$$

$$\times (-\coth_O(2\rho\vartheta) \pm \sqrt{mn}\operatorname{sech}_O(2\rho\vartheta)),$$
(42)

$$K_{30}(x,t) = \sqrt{3} \sqrt{\frac{\ell}{2j(1 - 2\ell\mu^2 \ln(Q)^2 \rho^2)}} \ln(Q)\mu\rho$$

$$\times \left[ \tanh_Q \left( \frac{\rho}{2} \vartheta \right) + \coth_Q \left( \frac{\rho}{2} \vartheta \right) \right]. \tag{43}$$

(Class 7), (Class 8), (Class 9), and (Class 10) offer consistent solutions.

(Class 11): As  $\rho = 0$  and  $\varpi \neq 0$ , a mixed hyperbolic solution was developed

$$K_{31}(x,t) = \sqrt{3} \sqrt{\frac{\ell}{j(2 - \ell \mu^2 \ln(Q)^2 \varpi^2)}} \ln(Q) \mu \varpi$$

$$\times \left[ 1 - \frac{2m}{(\cosh_Q(\varpi\vartheta) - \sinh_Q(\varpi\vartheta) + m)} \right], \tag{44}$$

$$K_{32}(x, t) = \sqrt{3} \sqrt{\frac{\ell}{j(2 - j\mu^2 \ln(Q)^2 \varpi^2)} \ln(Q) \mu \varpi} \times \left[1 - \frac{2(\sinh_Q(\varpi\vartheta) + \cosh_Q(\varpi\vartheta))}{(\sinh_Q(\varpi\vartheta) + \cosh_Q(\varpi\vartheta) + n)}\right].$$
(45)

(Class 12): As  $\lambda = pq$ ,  $(q \neq 0)$ ,  $\varpi = p$ , along with  $\rho = 0$ , plane soliton outcome was obtained as

6 — Dean Chou et al. DE GRUYTER

$$K_{33}(x,t) = \sqrt{3} \sqrt{\frac{\ell}{\cancel{j}(2 - \ell \mu^2 \ln(Q)^2 P^2)}} \ln(Q) \mu P$$

$$\times \left[ 1 - \frac{2qmQ^{P\vartheta}}{m - qnQ^{P\vartheta}} \right]. \tag{46}$$

## 4 Graphical explanation

In this section, we present a comprehensive graphical illustration of the obtained soliton solutions by varying key system parameters. The analysis reveals a diverse range

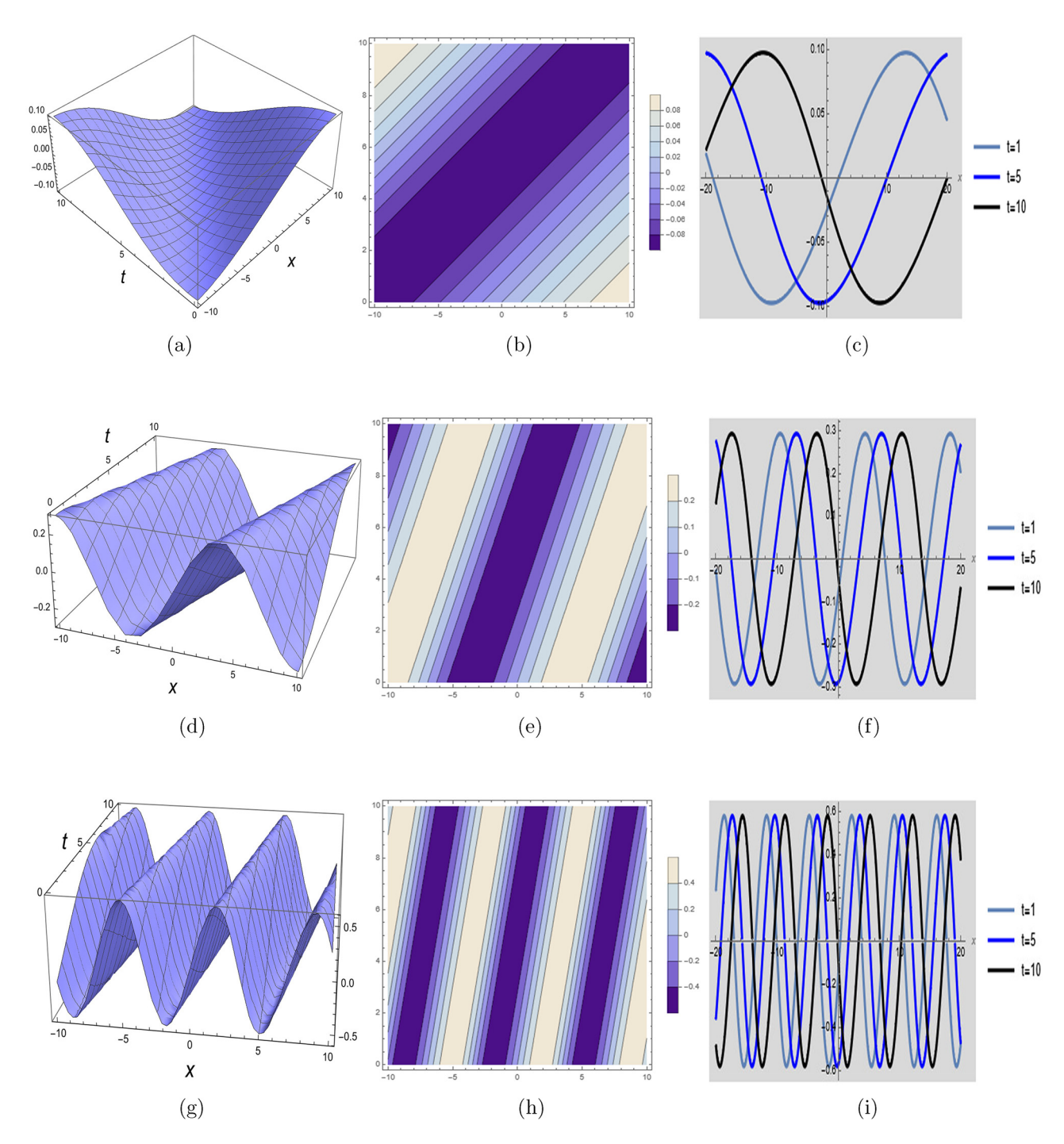


**Figure 1:** Three-dimensional, two-dimensional, and contour plots of the dark compacton soliton solution  $K_1(x, t)$ . (a) 3D visualization at  $\mu = 0.1$ , (b) contour visualization at  $\mu = 0.1$ , (c) 2D visualization at  $\mu = 0.1$ , (d) 3D visualization at  $\mu = 0.3$ , (e) contour visualization at  $\mu = 0.3$ , (f) 2D visualization at  $\mu = 0.3$ , (g) 3D visualization at  $\mu = 0.6$ , (h) contour visualization at  $\mu = 0.6$ , and (i) 2D visualization at  $\mu = 0.6$ .

of wave structures, including periodic waves, shock waves, singular waves, and complex solitary shock solutions. Among these, singular soliton solutions exhibit unique characteristics that distinguish them from conventional solitons. Such solutions play a crucial role in describing

wave phenomena that maintain coherence over long distances, resisting dispersion. These results have broad applications in nonlinear wave dynamics, including optical solitons in fiber optics and water solitons in hydrodynamics.

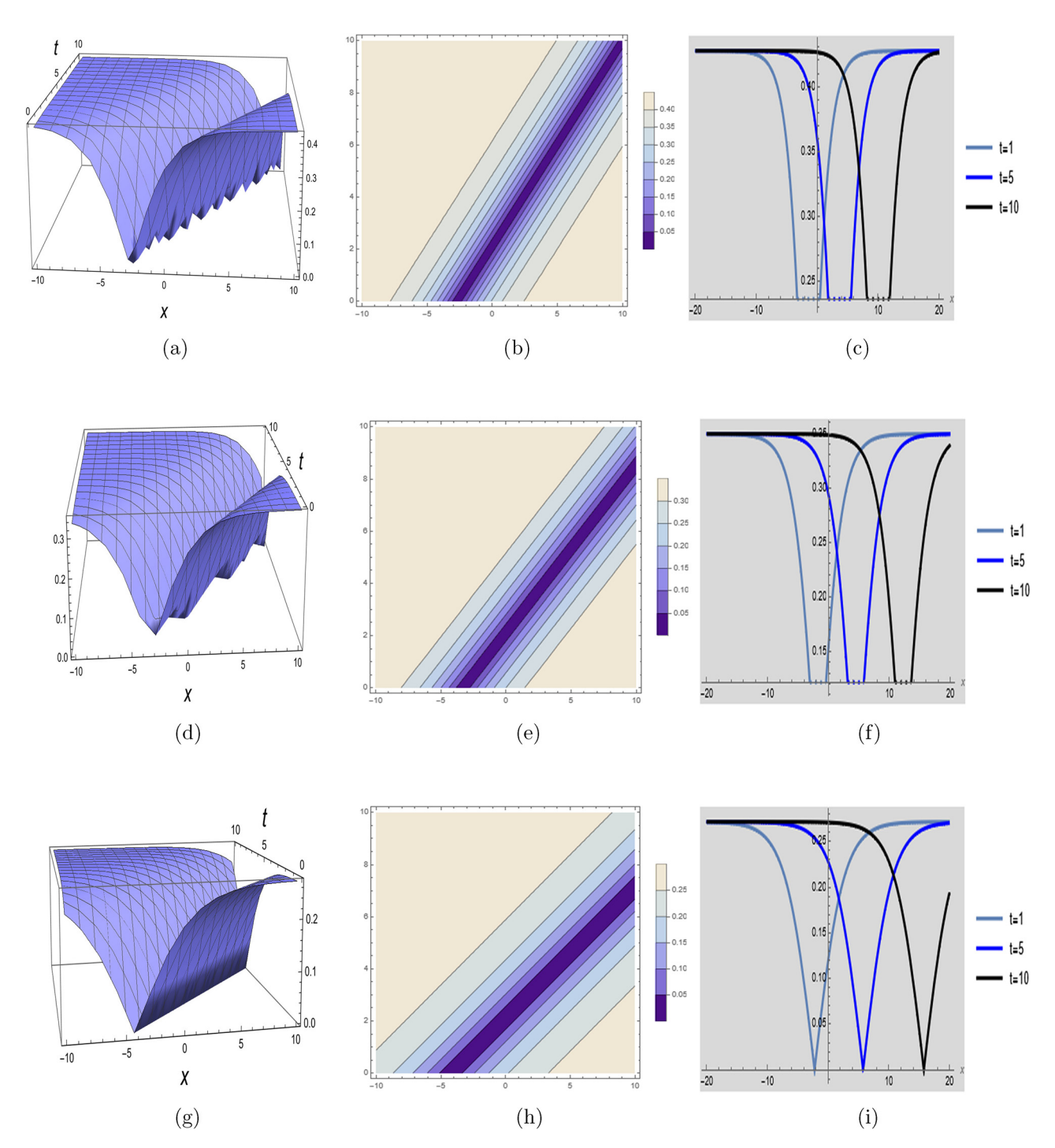


**Figure 2:** Three-dimensional, two-dimensional, and contour plots of the dark compacton soliton solution  $K_6(x, t)$ . (a) 3D visualization at  $\mu = 1.1$ , (b) Contour visualization at  $\mu = 1.1$ , (c) 2D visualization at  $\mu = 1.1$ , (d) 3D visualization at  $\mu = 0.9$ , (e) contour visualization at  $\mu = 0.9$ , (f) 2D visualization at  $\mu = 0.9$ , (g) 3D visualization at  $\mu = 0.7$ , (h) contour visualization at  $\mu = 0.7$ , and (i) 2D visualization at  $\mu = 0.7$ .

8 — Dean Chou et al. DE GRUYTER

To effectively demonstrate the behavior of the solutions, we provide a series of graphical representations in 3D, 2D, and contour plots, highlighting their dynamic properties under different parameter settings. The numerical values chosen for visualization are  $\ell=0.5$ ,  $\rho=0.7$ ,  $\mu=0.1$ , j=0.003, L=1.4,  $\nu=0.2$ , m=0.05, n=0.9, Q=15, m=1.9.

Therefore, these graphical representations of our most recent findings should be beneficial for the scientific analysis and precise prediction of outcomes for nonlinear wave problems. Figure 1 expresses the compacton (dark compacton) of  $K_1(x,t)$  at values of  $\mu=0.1$  as well as obtaining the combined bright-dark soliton at the values

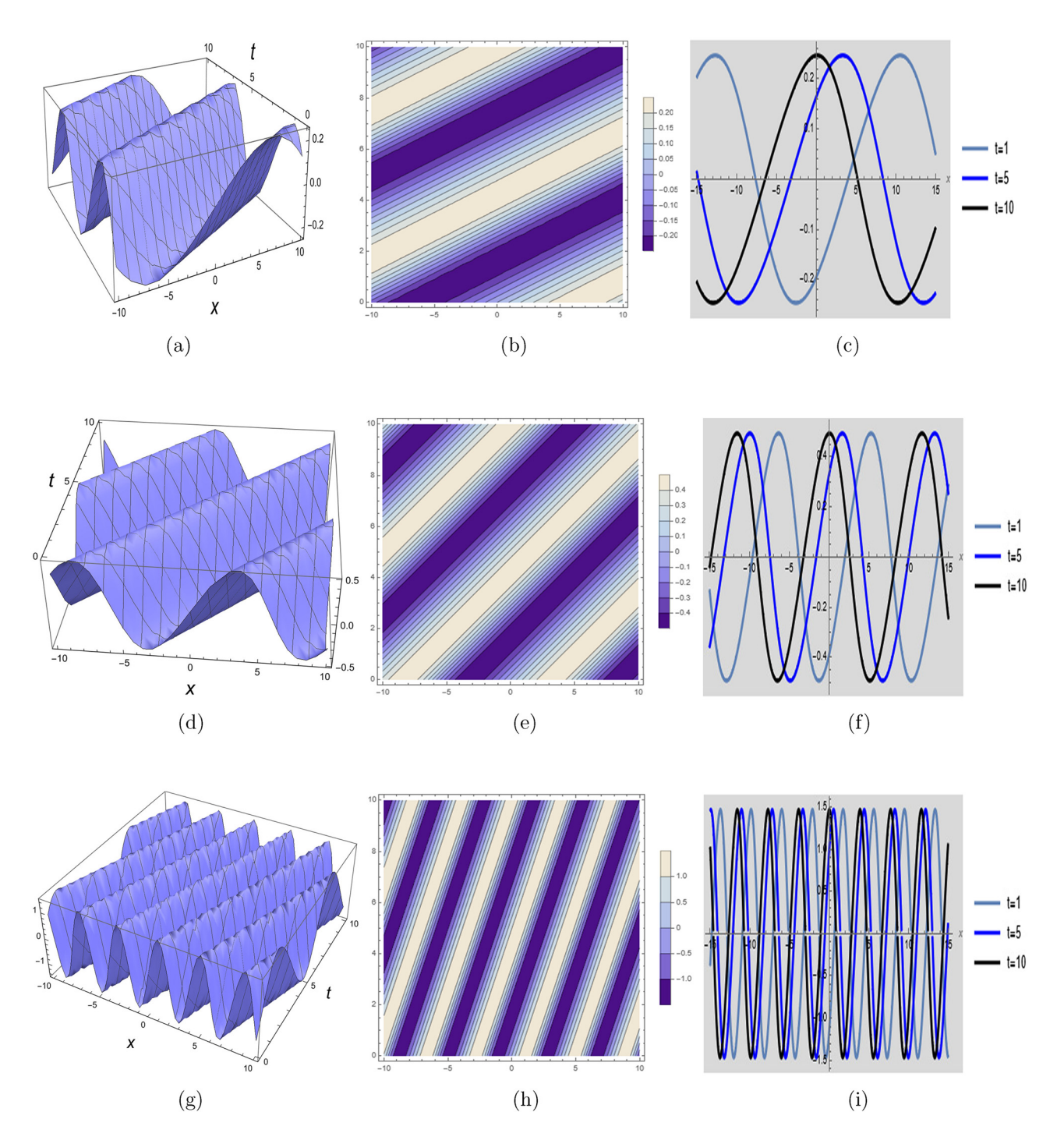


**Figure 3:** Three-dimensional, two-dimensional, and contour plots of the combined bright-dark soliton solution  $K_{11}(x, t)$ . (a) 3D visualization at  $\mu = 0.05$ , (b) contour visualization at  $\mu = 0.05$ , (c) 2D visualization at  $\mu = 0.05$ , (d) 3D visualization at  $\mu = 0.1$ , (e) contour visualization at  $\mu = 0.1$ , (g) 3D visualization at  $\mu = 0.3$ , (h) contour visualization at  $\mu = 0.3$ , and (i) 2D visualization at  $\mu = 0.3$ .

of  $\mu$  = 0.3 and  $\mu$  = 0.6. Figure 2 expresses the multi-peak with decay of  $K_6(x,t)$  at value of  $\mu$  = 1.1 and obtaining the anti-peaked with decay at the values of  $\mu$  = 0.9 and  $\mu$  = 0.7. Figure 3 expresses the combined bright-dark soliton of  $K_{11}(x,t)$  at values of  $\mu$  = 0.05,  $\mu$  = 0.1,  $\mu$  = 0.3. Figure 4

expresses the multi peak with decay of  $K_{16}(x, t)$  at values of  $\mu = 0.5$ ,  $\mu = 0.7$ ,  $\mu = 0.9$ .

These enhanced graphical representations not only validate the analytical findings but also provide a significant contribution to the study of nonlinear wave propagation. The results are of

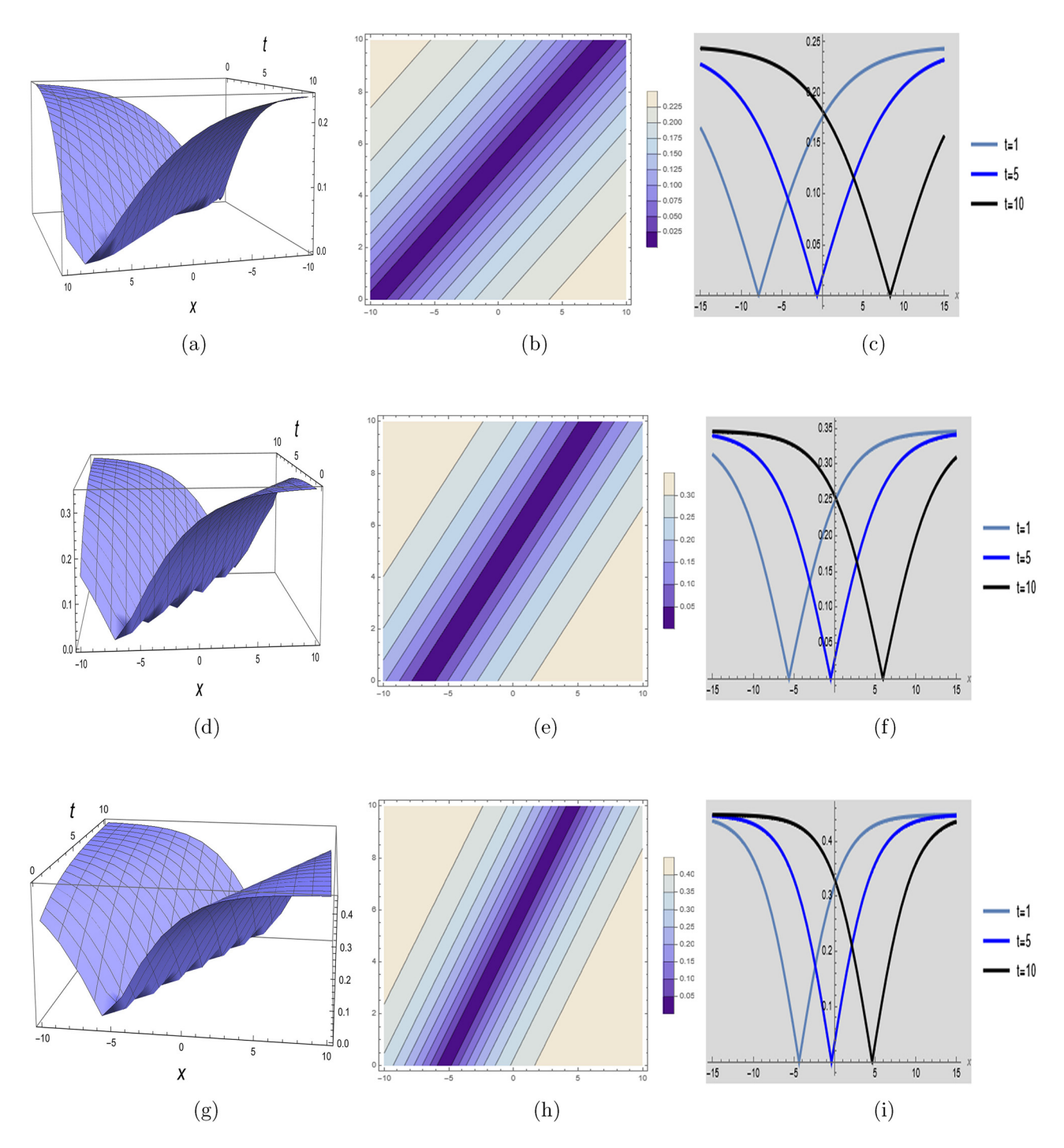


**Figure 4:** Three-dimensional, two-dimensional, and contour plots of the multi peak with decay soliton solution  $K_{16}(x, t)$ . (a) 3D visualization at  $\mu = 0.5$ , (b) contour visualization at  $\mu = 0.5$ , (c) 2D visualization at  $\mu = 0.5$ , (d) 3D visualization at  $\mu = 0.7$ , (e) contour visualization at  $\mu = 0.7$ , (f) 2D visualization at  $\mu = 0.7$ , (g) 3D visualization at  $\mu = 0.9$ , (h) contour visualization at value of  $\mu = 0.9$ , and (i) 2D visualization at value of  $\mu = 0.9$ .

paramount importance to physicists, chemists, and engineers, offering valuable insights for industrial applications and advancing research in soliton theory. To further improve clarity and interpretation, all figures must be optimized to emphasize the main physical significance of the governing model, ensuring a clearer understanding of the underlying wave dynamics.

### 5 Dynamical visualization

This portion presents the dynamical insights of the mBBM equation. To accomplish this goal, sensitive analyses are employed. The planar dynamical technique is derived using the Galilean transformation [53,54],

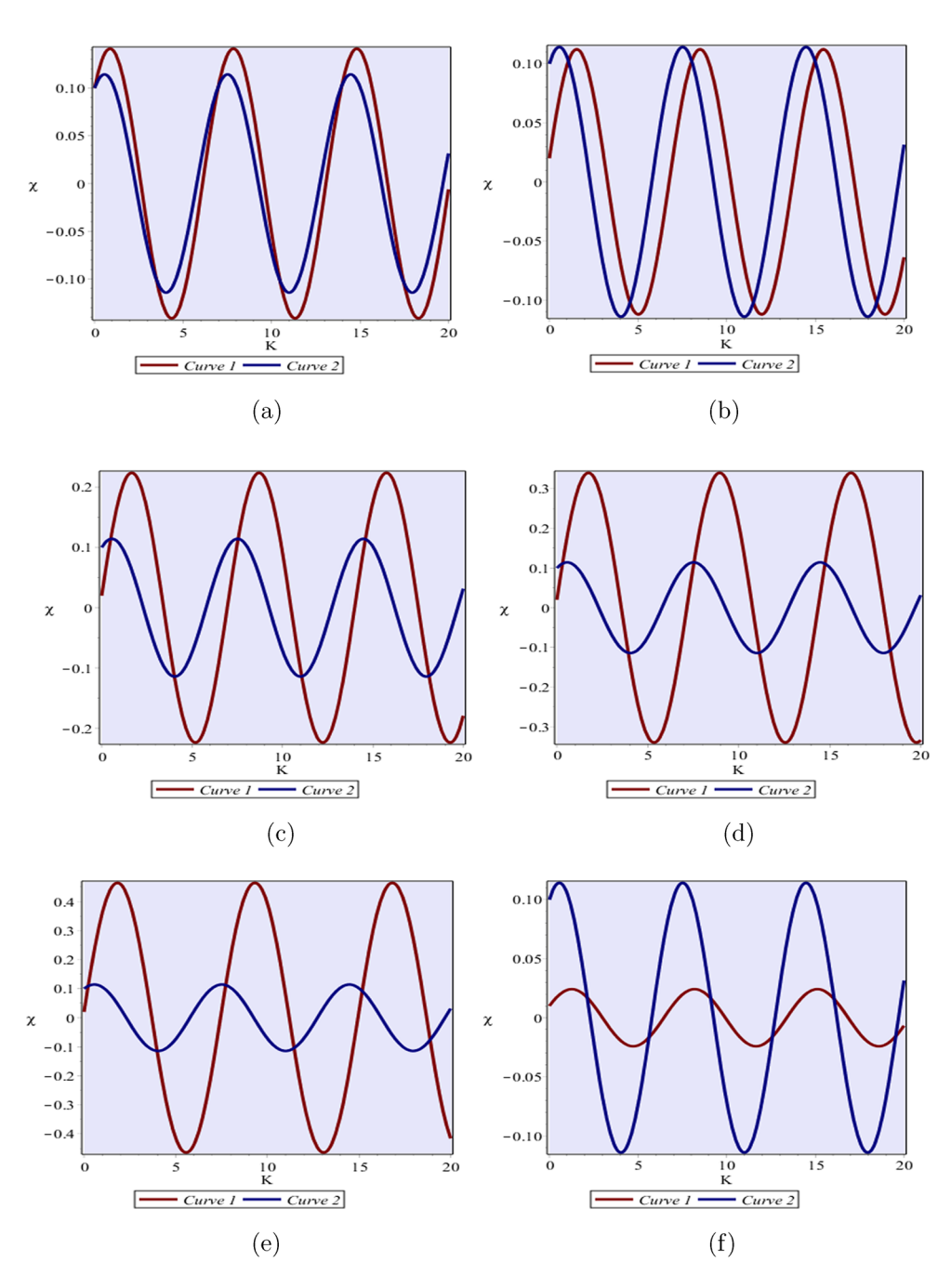


**Figure 5:** Sensitivity visualization based on different initial values. (a) Visualizing sensitivity along curve 1 and curve 2 for the points (0.1, 0.09) and (0.1, 0.05), (b) sensitive representation over curve 1 and curve 2, for (0.02, 0.1) and (0.1, 0.05), (c) visualizing sensitivity along curve 1 and curve 2 for the points (0.02, 0.2) and (0.1, 0.05), (d) visualizing sensitivity along curve 1 and curve 2 for the points (0.02, 0.3) and (0.1, 0.05), (e) visualizing sensitivity along curve 1 and curve 2 for the points (0.02, 0.4) and (0.1, 0.05), and (f) visualizing sensitivity along curve 1 and curve 2 for the points (0.01, 0.02) and (0.1, 0.05).

$$\begin{cases} \frac{\mathrm{d}K}{\mathrm{d}\vartheta} = \chi, \\ \frac{\mathrm{d}\chi}{\mathrm{d}\vartheta} = \frac{1}{\mu^2 \nu \ell} \left[ (\mu - \nu)K + \frac{1}{3}\mu K^3 \right]. \end{cases}$$
(47)

Particular importance is the fact that the planar dynamical technique (47) embodies a planar Hamiltonian structure. Through integration, one can ensure the presence of a dynamical system's Hamiltonian function (47),

$$\mathfrak{R} = \frac{\lambda^2}{2} - \frac{1}{\mu^2 \nu \ell} \left[ (\mu - \nu) \frac{K^2}{2} + \frac{1}{12} \mu K^4 \right]. \tag{48}$$

One can verify from (48) that

$$\frac{\mathrm{d}K}{\mathrm{d}\vartheta} = \frac{\partial \Re}{\partial \chi} \quad \text{and} \quad \frac{\mathrm{d}\chi}{\mathrm{d}\vartheta} = -\frac{\partial \Re}{\partial K}.$$
 (49)

As per the argument regarding system (49), the planar dynamical technique for Eq. (47) is a Hamiltonian structure. Furthermore, system (47) serves as a generalized form that includes all the traveling wave solutions derived in this study Asghar et al. [55]. Dynamical visualization generally refers to the creation and display of visual representations that convey changes or movements over time.

#### 5.1 Sensitive assessment

This section describes the planer dynamical system's (47) sensitive behavior to check out the sensitivity of the governing model. The sensitive analysis is performed taking into account the parametric values  $\mu = 0.09$ ,  $\nu = 0.1$ , l = 15, j = 0.1.

One can note from Figure 5 that little modifications in the initial variables have a huge influence on the model's behavior. This signifies that the algorithm is sensitive to the starting value.

#### 6 Conclusion

This study provides a comprehensive analytical investigation of the mBBM equation, employing the new extended direct algebraic approach to derive a broad spectrum of solitonic solutions. The proposed methodology successfully generates distinct and generalized solutions, categorized into 12 classes, including rational, hyperbolic, and trigonometric functions, as well as mixed singular, shock-singular, complex solitary-shock, periodic, trigonometric, hyperbolic, and plane wave solutions. These analytical solutions offer deeper insights into the nonlinear dynamics of the model, reinforcing the significance of algebraic techniques

in solving complex NPDEs. The solutions obtained are crucial for modeling various physical phenomena, especially in optical pulse transmission interactions. The study also establishes the conservation properties of the system through the Hamiltonian function, demonstrating that the mass and energy remain conserved. Furthermore, sensitivity analysis reveals that the system is highly responsive to initial conditions, emphasizing the need for precise parameter selection in practical applications. The propagation behavior of solitons and the dynamical characteristics of the model are visually represented through 3D, 2D, and contour plots. In general, this study contributes to the growing body of research on nonlinear wave equations, providing a robust analytical framework for future studies in soliton theory and mathematical physics.

Acknowledgments: The authors gratefully acknowledge the support from the National Science and Technology Council (NSTC), Taiwan, under Project No. 113-2221-E-006-033-MY3. We also thank the Yushan Fellow Program (Project No. MOE-113-YSFEE-0005-001-P1) by the Ministry of Education (MOE), Taiwan, for the financial support.

Funding information: This research was financially supported by the National Science and Technology Council (NSTC), Taiwan, under Project No. 113-2221-E-006-033-MY3, and by the Yushan Fellow Program (Project No. MOE-113-YSFEE-0005-001-P1) of the Ministry of Education, Taiwan.

Author contributions: U. Asghar and M. I. Asjad conceptualization, methodology, and software, and validation, formal analysis. D. Chou, U. Asghar, and M. I. Asjad investigation, resources, writing original draft preparation, and visualization. D. Chou, U. Asghar, and M. I. Asjad, supervision, and project administration. All authors have accepted responsibility for the entire content of this manuscript and approved its submission.

Conflict of interest: The authors state no conflict of interest.

Data availability statement: Data sharing does not apply to this article as no data sets were generated or analyzed during the current study.

#### References

Jin S, Liu N, Yu Y. Time complexity analysis of quantum algorithms via linear representations for nonlinear ordinary and partial differential equations. J Comp Phys. 2023;487:112149.

- [2] Rezazadeh H, Inc M, Baleanu D. New solitary wave solutions for variants of (3+1)-dimensional Wazwaz-Benjamin-Bona-Mahony equations. Fron Phys. 2020;8:332.
- [3] Zhou G, Xu J, Hu H, Liu Z, Zhang H, Xu C, et al. Off-axis fourreflection optical structure for lightweight single-band bathymetric LiDAR. IEEE Trans on Geo and Rem Sens. 2023;61:1-17.
- Dong Y, Li W, Zhang J, Luo W, Fu H, Xing X. High-speed PGC demodulation model and method with subnanometer displacement resolution in a fiber-optic micro-probe laser interferometer. Phot Res. 2024;12(5):921-31.
- Riaz MB, Jhangeer A, Kazmi SS. Optical soliton stability in zig-zag optical lattices: comparative analysis through two analytical techniques and phase portraits. Non Dyna. 2024;112(24):22221-43.
- Sagib M, Seadawy AR, Khaliq A, Rizvi ST. Efficiency and stability analysis on nonlinear differential dynamical systems. Int | Mod Phy B. 2023;37(10):2350098.
- Dong C, Fu Q Wang K, Zong F, Li M, He Q. The model and characteristics of polarized light transmission applicable to polydispersity particle underwater environment. Opt Las Eng. 2024;182:108449.
- Dhiman SK, Kumar S. Analyzing specific waves and various dynamics of multi-peakons in (3+1)-dimensional p-type equation using a newly created methodology. Non Dyna. 2024;112(12):10277-90.
- Shi J, Liu C, Liu J. Hypergraph-based model for modelling multiagent q-learning dynamics in public goods games. IEEE Tran Net Sci Eng. 2024;11(6):6169-79.
- [10] Yao SW, Tarig KU, Inc M, Tufail RN. Modulation instability analysis and soliton solutions of the modified BBM model arising in dispersive medium. Resul Phy. 2023;46:106274.
- [11] Qiao C, Long X, Yang L, Zhu Y, Cai W. Calculation of a dynamical substitute for the real earth-moon system based on Hamiltonian analysis. Astro J. 2025;991(1):46.
- [12] Ahmed I, Seadawy AR, Lu D. M-shaped rational solitons and their interaction with kink waves in the Fokas-Lenells equation. Phys Scri. 2019;94(5):055205.
- [13] Booo Y, Tian D, Liu X, Jin Y. Discrete maximum principle and energy stability of the compact difference scheme for two-dimensional Allen-Cahn equation. J Funct Spa. 2022(1):8522231.
- [14] Wang A, Cheng C, Wang L. On r-invertible matrices over antirings. Public Math Debr. 2025:106(3-4):445-59.
- [15] Zhou G, Liu J, Gao K, Liu R, Tang Y, Cai A. A coupling method for the stability of reflectors and support structure in an ALB opticalmechanical system. Remo Sens. 2024;17(1):60.
- [16] Sun YL, Ma WX, Yu JP. N-soliton solutions and dynamic property analysis of a generalized three-component Hirota-Satsuma coupled KdV equation. Appl Math Let. 2021;120:107224.
- [17] Kaur L, Wazwaz AM. Optical soliton solutions of variable coefficient Biswas-Milovic (BM) model comprising Kerr law and damping effect. Opt. 2022;266:169617.
- [18] Mahdy AMS, Lotfy K, Hassan W, El-Bary AA. Analytical solution of magneto-photothermal theory during variable thermal conductivity of a semiconductor material due to pulse heat flux and volumetric heat source. Wav Rand Comp Med. 2021;31(6):2040-57.
- [19] Khamis AK, Lotfy K, El-Bary AA, Mahdy AM, Ahmed MH. Thermalpiezoelectric problem of a semiconductor medium during photothermal excitation. Wav Ran Comp Med. 2021;31(6):2499-513.
- [20] Osman MS, Rezazadeh H, Eslami M, Neirameh A, Mirzazadeh M. Analytical study of solitons to Benjamin-Bona-Mahony-Peregrine

- equation with power law nonlinearity by using three methods. Univ Polit Bucharest Sci Bulletin-Ser A-App Math Phys. 2018;80(4):267-78.
- [21] Yokus A, Sulaiman TA, Bulut H. On the analytical and numerical solutions of the Benjamin-Bona-Mahony equation. Opt Quan Elect. 2018;50(1):31.
- [22] Sun ED, Dekel R. ImageNet-trained deep neural networks exhibit illusion-like response to the Scintillating grid. J Vis. 2021:21(11):15.
- [23] Coclite GM, diRuvo L. On the convergence of the modified Rosenau and the modified Benjamin-Bona-Mahony equations. Comp Math Appl. 2017;74(5):899-919.
- [24] Asghar U, Faridi WA, Asjad MI, Eldin SM. The enhancement of energy-carrying capacity in liquid with gas bubbles, in terms of solitons. Symm. 2022:14(11):2294.
- [25] Faridi WA, Asghar U, Asjad MI, Zidan AM, Eldin SM. Explicit propagating electrostatic potential waves formation and dynamical assessment of generalized Kadomtsev-Petviashvili modified equal width-Burgers model with sensitivity and modulation instability gain spectrum visualization. Res Phys. 2023;44:106167.
- [26] Seadawy AR, Cheemaa N. Applications of extended modified auxiliary equation mapping method for high-order dispersive extended nonlinear Schrödinger equation in nonlinear optics. Mod Phys Let B. 2019;33(18):1950203.
- [27] Asghar U, Asjad MI, Faridi WA, Muhammad T. The conserved vectors and solitonic propagating wave patterns formation with Lie symmetry infinitesimal algebra. Opt Quant Electron. 2024;56(4):540.
- [28] Seadawy A. Stability analysis of traveling wave solutions for generalized coupled nonlinear KdV equations. Appl Math Info Sci. 2016;10(1):209.
- [29] Kumar V. Modified (G'/G)-expansion method for finding traveling wave solutions of the coupled Benjamin-Bona-Mahony-KdV equation. J Ocean Eng Scie. 2019;4(3):252-5.
- [30] Kadem DAA. Application of the extended Fan sub-equation method to time fractional burgers-fisher equation. Tatra Mt Math Publ. 2021:79:1-12.
- [31] Rizvi ST, Seadawy AR, Ahmed S, Ashraf R. Lax pair, Darboux transformation, Weierstrass-Jacobi elliptic and generalized breathers along with soliton solutions for Benjamin-Bona-Mahony eguation. Int | Mod Phys B. 2023;37(24):2350233.
- [32] Khalil TA, Badra N, Ahmed HM, Rabie WB, Optical solitons and other solutions for coupled system of nonlinear Biswas-Milovic equation with Kudryashovas law of refractive index by Jacobi elliptic function expansion method. Opt. 2022;253:168540.
- [33] Elmandouh A, Fadhal E. Bifurcation of exact solutions for the spacefractional stochastic modified Benjamin-Bona-Mahony equation. Frac Frac. 2022;6(12):718.
- [34] Jhangeer A, Hussain A, Junaid-U-Rehman M, Baleanu D, Riaz MB. Quasi-periodic, chaotic and travelling wave structures of modified Gardner equation. Chas Soli Frac. 2023;143:110578.
- [35] Rahan NNM, Hamid NNA, Majid AA, Ismail AIM. Cubic B-spline collocation method for solving Benjamin-Bona-Mahony equation. AIP Conf Proc. 2019;218:4060020.
- [36] Babajanov B, Abdikarimov F, Solitary and periodic wave solutions of the loaded modified Benjamin-Bona-Mahony equation via the functional variable method. Res Math. 2022;30(1):10-20.
- [37] Yan XW, Tian SF, Dong MJ, Wang XB, Zhang TT. Nonlocal symmetries, conservation laws and interaction solutions of the generalised dispersive modified Benjamin-Bona-Mahony equation. Zeit für Natu A. 2018;73(5):399-405.

- [38] Gündoğdu H, Gözükızıl ÖF. Solving Benjamin-Bona-Mahony equation by using the sn-ns method and the tanh-coth method. Math Mora. 2017;21(1):95–103.
- [39] Alsayyed O, Jaradat HM, Jaradat MMM, Mustafa Z. Multi-soliton solutions of the BBM equation arisen in shallow water. J Nonlinear Sci Appl. 2016;9(4):1807–14.
- [40] Alhamud M, Elbrolosy M, Elmandouh A. New analytical solutions for time-fractional stochastic (3+1)-dimensional equations for fluids with gas bubbles and hydrodynamics. Frac Frac. 2022;7(1):16.
- [41] Mohammed WW, Al-Askar FM, Cesarano C. The analytical solutions of the stochastic mKdV equation via the mapping method. Math. 2022;10(22):4212.
- [42] Al-Askar FM. Mohammed WW. The analytical solutions of the stochastic fractional RKL equation via Jacobi elliptic function method. Adv Math Phys. 2022;(1):1534067.
- [43] Riaz MB, Jhangeer A, Kozubek T, Kazmi SS. Investigating multisoliton patterns and dynamical characteristics of the (3+1)dimensional equation via phase portraits. Par Diff Eqs App Math. 2024:12:100926.
- [44] Ege SM, Misirli E. The modified Kudryashov method for solving some fractional-order nonlinear equations. Adv Diff Eqs. 2014;1:135.
- [45] Rabie WB, Ahmed HM. Cubic-quartic optical solitons and other solutions for twin-core couplers with polynomial law of nonlinearity using the extended F-expansion method. Opt. 2022;253:168575.
- [46] Darwish A, Ahmed HM, Arnous AH, Shehab MF. Optical solitons of Biswas-Arshed equation in birefringent fibers using improved modified extended tanh-function method. Opt. 2021;227:165385.
- [47] Rabie WB, Ahmed HM. Dynamical solitons and other solutions for nonlinear Biswas-Milovic equation with Kudryashovas law by

- improved modified extended tanh-function method. Opt. 2021:245:167665.
- [48] Ahmed MS, Zaghrout AA, Ahmed HM. Travelling wave solutions for the doubly dispersive equation using improved modified extended tanh-function method. Alex Eng J. 2022;61(10):7987–94.
- [49] Seadawy AR, Ahmed HM, Rabie WB, Biswas A. An alternate pathway to solitons in magneto-optic waveguides with triple-power law nonlinearity. Opt. 2021;231:166480.
- [50] Shakeel M, Manan A, Turki NB, Shah NA, Tag SM. Novel analytical technique to find diversity of solitary wave solutions for Wazwaz-Benjamin-Bona Mahony equations of fractional order. Res Phys. 2023;51:106671.
- [51] Mahmood I, Hussain E, Mahmood A, Anjum A, Shah SAA. Optical soliton propagation in the Benjamin-Bona-Mahoney-Peregrine equation using two analytical schemes. Opt. 2023;287:171099.
- [52] Ghayad MS, Badra NM, Ahmed HM, Rabie WB. Derivation of optical solitons and other solutions for nonlinear Schrödinger equation using modified extended direct algebraic method. Alex Eng J. 2023;64:801–11.
- [53] Mann N, Kumar S. Dynamics of different soliton solutions, phase portraits, bifurcation analysis, and chaotic behavior in the Benney-Luke equation represent surface waves in a shallow channel with surface tension effects. Qual The Dyna Sys. 2025;24(4):1–30.
- [54] Kumar S, Kukkar A. Dynamics of several optical soliton solutions of a (3+1)-dimensional nonlinear Schrödinger equation with parabolic law in optical fibers. Mod Phys Let B. 2025;39(09):2450453.
- [55] Asghar U, Asjad MI, Faridi WA, Akgül A. Novel solitonic structure, Hamiltonian dynamics and lie symmetry algebra of biofilm. Par Diff Eqs App Math. 2025;9:100653.